Coherent Structural Dynamics and Electronic Correlations during an Ultrafast Insulator-to-Metal Phase Transition in VO_2

C. Kübler,[1] H. Ehrke,[1] R. Huber,[1,*] R. Lopez,[2,3] A. Halabica,[2] R. F. Haglund, Jr.,[2] and A. Leitenstorfer[1]

[1]*Department of Physics and Center for Applied Photonics, University of Konstanz, D-78457 Konstanz, Germany*

[2]*Department of Physics and Astronomy, Vanderbilt University, Nashville, Tennessee 37235, USA*

[3]*Department of Physics and Astronomy and Institute of Advanced Materials, Nanoscience and Technology, University of North Carolina, Chapel Hill, North Carolina 27599, USA*

(Received 14 November 2006; published 13 September 2007)

We directly trace the multi-THz conductivity of VO_2 during an insulator-metal transition triggered by a 12-fs light pulse. The femtosecond dynamics of lattice and electronic degrees of freedom are spectrally discriminated. A coherent wave packet motion of V-V dimers at 6 THz modulates the lattice polarizability for approximately 1 ps. In contrast, the electronic conductivity settles to a constant value already after one V-V oscillation cycle. Based on our findings, we propose a qualitative model for the nonthermal phase transition.

DOI: 10.1103/PhysRevLett.99.116401 PACS numbers: 71.30.+h, 72.80.Ga, 78.47.+p

Metal-insulator transitions in strongly correlated electron systems are among the most intriguing phenomena in condensed-matter physics [1]. A delicate balance of cooperative interactions of crystal structure and electronic degrees of freedom drives the materials into a critical regime. Vanadium dioxide (VO_2) is a prime example: It undergoes a first-order transition from a high-temperature metallic to a low-temperature insulating phase at $T_c = 340$ K [2], while the crystal symmetry is reduced from rutile (R) to monoclinic ($M1$) due to dimerization of V atoms. The driving force of this transition has been a topic of controversy. Both a structural Peierls instability with a bandlike energy gap in the $M1$ phase [3,4], as well as Coulomb repulsion and charge localization typical of a Mott insulator [5–7] have been proposed.

Time-resolved studies, using femtosecond light pulses to photoinject electron-hole pairs into VO_2 and trigger an insulator-metal transition combined with structural rearrangement, have promised insight into the microscopic dynamics [8–10]. Optical [10–13], x-ray [9], and photoemission [14] spectroscopies have been employed to follow ultrafast phase transitions. For VO_2, sufficient temporal resolution to reveal the inherent time scales has been reported only in femtosecond optical reflectivity data. They suggest a 75 fs structural bottleneck for photoswitching [10]. However, the microscopic dynamics remains elusive for visible light pulses. In contrast, unraveling the interplay of lattice and electronic structure requires *direct* and *selective access* to the respective microscopic degrees of freedom (DOF). Ultrabroadband THz pulses have recently been shown to couple directly to lattice polarizability as well as electronic conductivity, that is an order parameter of the ultrafast insulator-metal transition, on the femtosecond time scale [15].

Here, we report the first multi-THz measurements of VO_2 monitoring a femtosecond insulator-metal transition initiated by a 12-fs laser pulse. The mid-infrared (IR) conductivity simultaneously resolves the spectral signatures of electronic and ionic DOF, revealing fundamentally different dynamics. The lattice polarizability is strongly influenced by a coherent modulation at 6 THz characteristic of impulsively excited wave packet motion of V-V dimers. Depending on the excitation density, the electronic conductivity shows signatures either of excitonic self-trapping or an ultrafast crossover into a metallic phase. We propose a qualitative model explaining the dynamics.

The sample is a 120 nm thin film of polycrystalline VO_2 on a CVD diamond window [16,17]. Our multi-THz setup is based on a low-noise Ti:sapphire amplifier generating intense 12-fs light pulses with a center photon energy of 1.55 eV, at a repetition rate of 800 kHz [18]. Part of the output photoexcites the VO_2 film while another portion generates multi-THz pulses by optical rectification in GaSe [19]. These transients are transmitted through the sample held at a preset substrate temperature T_L. Phase-matched electro-optic sampling [20] yields amplitude and phase of the probe electric field in the time domain for selected delay times τ between excitation of the film and electro-optic detection of its response [21]. This two-dimensional (2D) multi-THz scheme provides direct access to the complex valued ultrabroadband conductivity $\sigma(\omega)$ and, simultaneously, to its pump-induced changes $\Delta\sigma(\omega, \tau)$ with femtosecond temporal resolution [15,21].

Figure 1(a) shows the real part $\sigma_1(\omega)$ of the THz conductivity of the unexcited VO_2 film below and above T_c. The large value and the spectral shape of $\sigma_1(\omega)$ in the metallic phase are consistent with mid-IR data in Ref. [22]. Although the electronic conductivity of insulating VO_2 should vanish, $\sigma_1(\omega)$ at $T_L = 295$ K exhibits three pronounced maxima at $\hbar\omega = 50$, 62, and 74 meV, corresponding to the polarizability of the highest-frequency transverse optical phonons associated with vibrations of the oxygen cages surrounding the V atoms [23]. The spectral region above 85 meV is free of IR-active resonances and thus

 © 2007 The American Physical Society

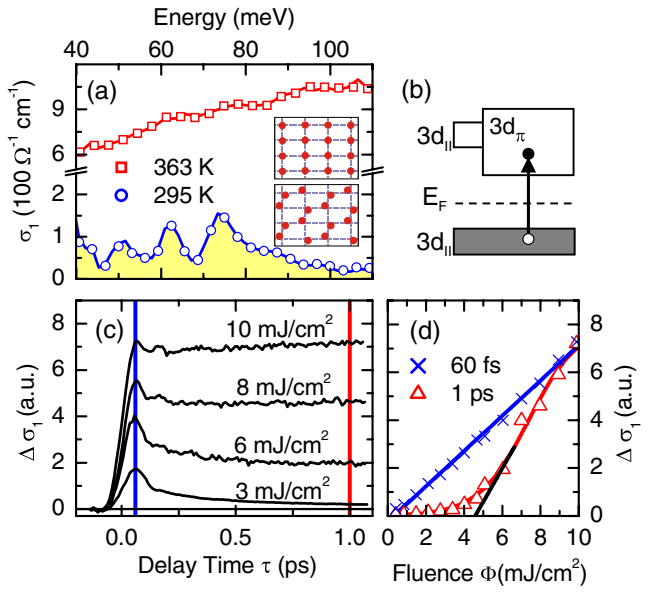

FIG. 1 (color online). (a) Mid-IR conductivity spectra of VO_2 at $T_L = 295$ K (blue circles) and 363 K (red squares). Inset: V sublattice of the R (upper part) and $M1$ (lower part) phase. (b) Schematic of photodoping in the insulating band structure of VO_2. (c) Spectrally integrated transient change of the THz conductivity after excitation at various fluences ($T_L = 295$ K). (d) Fluence dependence of $\Delta\sigma_1(\tau)$ at $\tau = 60$ fs (blue crosses) and 1 ps (red triangles). A linear fit to the latter graph extrapolates to a critical fluence $\Phi_c = 4.6$ mJ/cm^2.

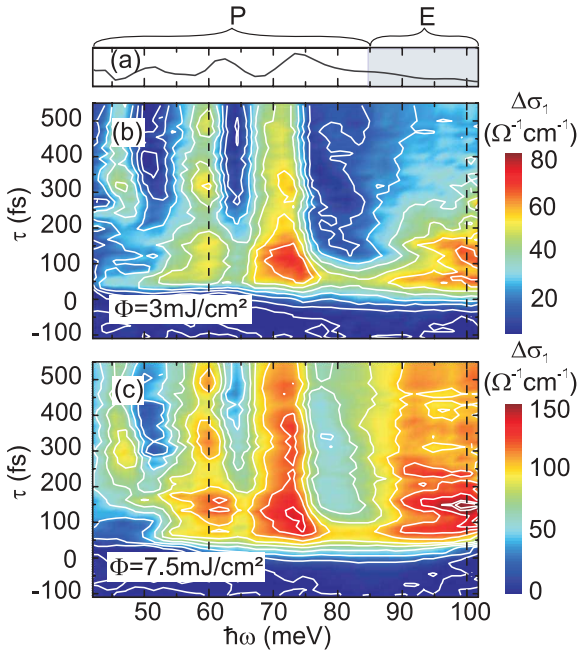

FIG. 2 (color online). 2D optical pump—THz probe data: (a) equilibrium conductivity of insulating VO_2 [from Fig. 1(a)]. (b) and (c): Color plot of the pump-induced *changes* of the conductivity $\Delta\sigma_1(\omega, \tau)$ for pump fluences (b) $\Phi = 3$ mJ/cm$^2 < \Phi_c$ and (c) $\Phi = 7.5$ mJ/cm$^2 > \Phi_c$ at $T_L = 250$ K. The broken vertical lines indicate the frequency positions of cross sections reproduced in Fig. 3. Spectral domain P comprises predominantly changes of the phonon resonances; region E reflects the electronic conductivity.

exhibits a THz conductivity almost 2 orders of magnitude lower than in the R phase.

We now perturb the insulating phase ($T_L = 295$ K) by ultrafast photo-excitation of electrons from the occupied $d_\parallel$ band into conduction-band states [Fig. 1(b)]. Figure 1(c) displays the subsequent ultrafast dynamics of the *spectrally integrated* conductivity change $\Delta\sigma_1(\tau)$, for a series of pump fluences. At low excitation densities, a sharp onset in the pump-induced signal is followed by a nonexponential sub-ps decay. Fluences above $\Phi_c = 4.6$ mJ/cm^2 generate an increasing background of long-lived conductivity that remains constant within a time window of 10 ps (not shown). Figure 1(d) summarizes the fluence dependence of $\Delta\sigma_1(\tau)$ for two characteristic early delay times. The quasi-instantaneous signal at $\tau = 60$ fs scales linearly with Φ. Hence, we attribute this feature to the conductivity of directly photoinjected carriers. In contrast, the corresponding value at $\tau = 1$ ps displays threshold behavior: The THz conductivity vanishes below Φ_c, while it grows nonlinearly above, indicating a cooperative ultrafast insulator-metal transition. We find that Φ_c decreases with increasing lattice temperature, e.g. $\Phi_c(T_L = 250\ \text{K}) = 5.3$ mJ/cm^2 and $\Phi_c(T_L = 325\ \text{K}) = 3$ mJ/cm^2.

The interplay between lattice and electronic DOF is unveiled in a full 2D optical pump—multi-THz probe experiment. The contour plots of Fig. 2 depict the spectral shape of the conductivity changes $\Delta\sigma_1(\omega, \tau)$ as a function of time delay τ. Figure 2(b) shows data for an excitation density of $\Phi = 3$ mJ/cm$^2 < \Phi_c$ at $T_L = 250$ K. We consider two domains (labeled P and E in Fig. 2) that correspond to different physical processes: Since spectral region E ($\hbar\omega \geq 85$ meV) is free of phonon resonances [see Figs. 1(a) and 2(a)], the pump-induced THz conductivity in this region derives solely from *electronic* DOF. Features in the energy regime P (40 meV $< \hbar\omega <$ 85 meV) relate to the IR-active phonon resonances, exposing the dynamics of the *lattice* DOF.

The differing origins of the signals in the two spectral windows are underscored by qualitatively different temporal dynamics: Ultrafast photodoping induces a quasi-instantaneous onset of conductivity in region E due to directly injected mobile carriers. $\Delta\sigma_1(\omega, \tau)$ in region E decays promptly within 0.4 ps. In contrast, the phononic contribution (domain P) is more long lived. While the onset of the phononic response varies for the three modes, we find intriguing common features. Photoexcitation induces an increase of polarizability on the low-frequency side of each phonon resonance while a smaller change is seen on the blue wing. For all modes, the change in frequency is superimposed on a remarkable coherent modulation of $\Delta\sigma_1(\omega, \tau)$, along the pump-probe delay axis τ. This phenomenon is most notable at a THz photon

energy of 60 meV [vertical broken line in Fig. 2(b)]. The corresponding cross section for the 2D data is reproduced in Fig. 3(a). The Fourier transform of the oscillations along τ is centered at 6 THz [Fig. 4(a)]. Phonons in this frequency regime are critical to the metal-insulator transition of VO_2. In the ground state, A_g lattice modes associated with stretching and tilting of V-V dimers are found at 5.85 and 6.75 THz [10]. These vibrations map the $M1$ structure onto the R lattice [6].

Figure 2(c) displays results of the 2D THz experiment at excitation above the threshold fluence. For early delay times $\tau < 500$ fs, the spectral features in region P qualitatively resemble the corresponding region in Fig. 2(b), scaled by excitation density. On the other hand, the dynamics of the conductivity in window E differs profoundly: After the onset of $\Delta\sigma_1(\omega, \tau)$ due to photodoping, the electronic conductivity shows one cycle of modulation in phase with the coherent lattice motion and a distinct signal maximum occurs at a temporal delay of $\tau = 130$ fs [Fig. 3(b)]. Subsequently, the THz conductivity settles at a constant value for at least 10 ps, indicating the transition of the electronic system into a metallic phase. Remarkably, for $\tau > 130$ fs no more periodic modulation is imprinted on the electronic conductivity, while the data in region P demonstrate that the crystal lattice is still in a state of large-amplitude coherent oscillations [Fig. 3(a)]. For late delay times τ beyond 1 ps, the phononic differential transmission completely vanishes for excitation below threshold, indicating a return to the $M1$ configuration.

Currently, there is no comprehensive theoretical description of the ultrafast insulator-metal transition in VO_2. We propose a qualitative picture that is inspired by recent cluster dynamical mean field calculations approximating the dielectric phase as a molecular crystal of V-V dimers embedded in a matrix of oxygen octahedra [24]. This work demonstrated that the band gap arises from the strong correlations between two electrons on each singlet which are modeled in a basis of bonding and antibonding Heitler-London orbitals. The energy dependence of such states on the nuclear coordinate (i.e., V-V separation) is depicted schematically in Fig. 4(b). The minimum of the bonding energy surface defines the atomic position in the $M1$ phase. Absorption of a near-IR photon removes an electron from the bonding orbital, destabilizing the dimer, while the lattice site is left in an excited Franck-Condon state [marker (i) in Fig. 4(b)]. In an isolated molecule, the energy surface of the excited state would lead to dissociation. Because of the repulsion by the nearest neighbors, an energy minimum of the antibonding orbitals will be located near the R configuration by symmetry. Ultrafast photoexcitation thus launches a coherent structural deformation of excited dimers [marker (ii) in Fig. 4(b)] followed by oscillations at 6 THz around the new potential minimum [11,25].

From the known lattice constants of the R and $M1$ phase, we estimate changes of the V-V distance as large as 0.2 Å [26]. Such extreme deformations impose strong distortions on the surrounding oxygen octahedra and affect their elastic tensors. Our experiment directly demonstrates the influence of a coherent lattice motion on other phonon resonances: In region P of Fig. 2, an overall redshift of the oxygen modes attests to a modified average structure of the V-V dimers, while the coherent modulation at 6 THz reflects large-amplitude oscillations about the new potential minimum in the excited state [Fig. 4(a)]. The observation of a single modulation frequency instead of a doublet at 5.85 and 6.75 THz as in the paired and tilted ground state [10] further supports our interpretation of the mid-IR sig-

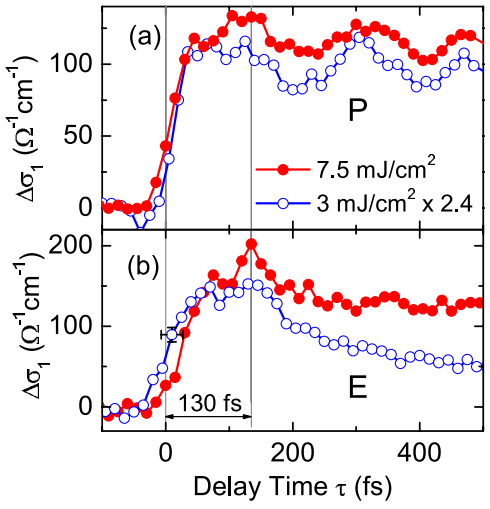

FIG. 3 (color online). Cross sections through the 2D data of Figs. 2(b) and 2(c) along the time axis τ for a photon energy of (a) $\hbar\omega = 60$ meV and (b) $\hbar\omega = 100$ meV. The traces taken at $\Phi = 3$ mJ/cm^2 are scaled by a factor of 2.4 in amplitude.

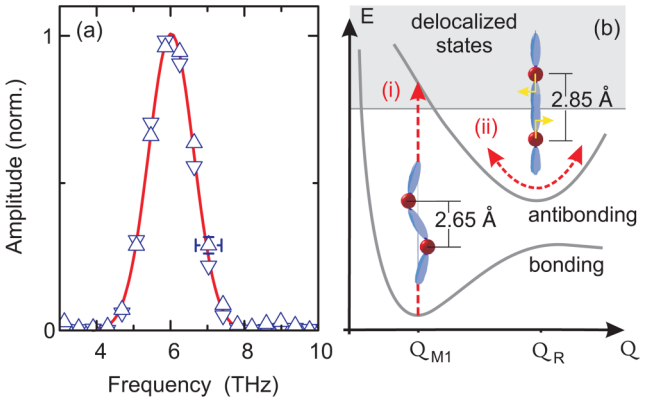

FIG. 4 (color online). (a) Fourier transform of the periodic modulation of the THz response in region P above ($\triangle$) and below ($\triangledown$) Φ_c. (b) Schematic potential surfaces of localized dimers. $\mathcal{Q}_{M1}$ and $\mathcal{Q}_R$ represent different spatial configurations of the V-V dimers in the structural phases $M1$ and R, respectively. (i) Photoexcitation of spin singlets into a conductive state. (ii) Structural relaxation and coherent vibrations about the new energy minimum.

nals originating from electronically excited lattice sites with higher symmetry.

Our tentative model also provides insight into the nature of the transient electronic conductivity. Photodoping initially leaves the electrons in a highly mobile state in the continuum of delocalized bands [Fig. 4(b)]. The rapid nonexponential decay of the electronic conductivity observed below Φ_c [Figs. 2(b) and 3(b)] indicates that the structural deformation shifts the energy of excited dimers below a mobility edge for extended electronic states—a process reminiscent of self-trapping of excitons [25].

In stark contrast, the electronic conductivity does not decay rapidly at high pump fluences. After an initial regime with one modulation cycle in parallel with the V-V coherent wave packet motion, the conductivity settles to a constant value with no more modulations discernible. Such behavior would be very surprising for a standard solid where the electronic system obeys the Born-Oppenheimer approximation and therefore reacts instantly to the lattice configuration. The decoupling of the electronic conductivity from the coherent lattice motion, which we observe after one V-V oscillation cycle, may be regarded as a direct consequence of the strongly correlated situation in the low-temperature phase of VO_2. Obviously, the local electronic correlations on each dimer that are the hallmark of the dielectric phase cannot be restored fast enough in the presence of a critical density of photoexcited lattice sites and thermal fluctuations preset by the substrate temperature. This retardation effect stabilizes the metallic conductivity already at a stage where the lattice is still far from equilibrium. Our model assumption of a reaction time of the local electron correlations that becomes slower than the V-V oscillation period might also explain why the metallic lattice configuration is ultimately adopted after excitation above threshold [9].

In conclusion, our femtosecond measurements of the mid-infrared complex dielectric function of VO_2 after ultrafast generation of electron-hole pairs suggest a novel qualitative picture for the photoinduced insulator-metal transition: In the earliest stage, the dynamics initiated by the femtosecond pulse starting in the dielectric phase resembles closely the local excitation of molecular V-V dimers into an antibonding state triggering a coherent wave packet motion of the stretching vibration. At moderate excitation fluences the strong correlations between the two binding electrons of each dimer are reestablished on a subpicosecond time scale and the mid-infrared electronic conductivity vanishes rapidly. However, if the density of excited lattice sites exceeds a bias-temperature dependent threshold, the situation changes dramatically. Local wave packet oscillations and thermal fluctuations drive the system to a point at which electronic correlations can no longer be restored. The mid-infrared electronic conductivity then settles close to the steady-state value characteristic of the metallic phase after approximately one V-V oscillation cycle, even though the lattice is still far from equilibrium. It will be interesting to see how future theoretical studies and further experimental work compare to our qualitative model. Similar phenomena may very well be relevant to a wider class of quantum phase transitions in other strongly correlated electron systems with spontaneous symmetry breaking in their ground states.

We thank I. Perakis, J. Kroha, Th. Dekorsy, A. Cavalleri, and J. Y. Suh for stimulating discussions and support. Research at Vanderbilt University is supported by the National Science Foundation (DMR0210785). R. F. H. gratefully acknowledges support from the Alexander von Humboldt Foundation.

*Corresponding author.
rupert.huber@uni-konstanz.de

[1] M. Imada *et al.*, Rev. Mod. Phys. **70**, 1039 (1998).
[2] F. J. Morin, Phys. Rev. Lett. **3**, 34 (1959).
[3] J. B. Goodenough, J. Solid State Chem. **3**, 490 (1971).
[4] R. M. Wentzcovitch *et al.*, Phys. Rev. Lett. **72**, 3389 (1994).
[5] A. Zylberstejn *et al.*, Phys. Rev. B **11**, 4383 (1975).
[6] D. Paquet *et al.*, Phys. Rev. B **22**, 5284 (1980).
[7] T. M. Rice *et al.*, Phys. Rev. Lett. **73**, 3042 (1994).
[8] M. F. Becker *et al.*, Appl. Phys. Lett. **65**, 1507 (1994).
[9] A. Cavalleri *et al.*, Phys. Rev. Lett. **87**, 237401 (2001); **95**, 067405 (2005).
[10] A. Cavalleri *et al.*, Phys. Rev. B **70**, 161102(R) (2004).
[11] H. J. Zeiger *et al.*, Phys. Rev. B **54**, 105 (1996).
[12] M. Chollet *et al.*, Science **307**, 86 (2005).
[13] S. Iwai *et al.*, Phys. Rev. Lett. **91**, 057401 (2003).
[14] L. Perfetti *et al.*, Phys. Rev. Lett. **97**, 067402 (2006).
[15] R. Huber *et al.*, Nature (London) **414**, 286 (2001).
[16] J. Y. Suh, J. Appl. Phys. **96**, 1209 (2004).
[17] Stoichiometry and phase transition are verified by Rutherford backscattering and IR transmission.
[18] R. Huber *et al.*, Opt. Lett. **28**, 2118 (2003).
[19] R. Huber *et al.*, Appl. Phys. Lett. **76**, 3191 (2000).
[20] C. Kübler *et al.*, Appl. Phys. Lett. **85**, 3360 (2004).
[21] J. T. Kindt *et al.*, J. Chem. Phys. **110**, 8589 (1999).
[22] H. S. Choi *et al.*, Phys. Rev. B **54**, 4621 (1996).
[23] P. Schilbe, Physica (Amsterdam) **316B**, 600 (2002).
[24] S. Biermann *et al.*, Phys. Rev. Lett. **94**, 026404 (2005).
[25] S. Dexheimer *et al.*, Phys. Rev. Lett. **84**, 4425 (2000).
[26] M. Marezio *et al.*, Phys. Rev. B **5**, 2541 (1972).